

# Relativistic Precession of Quantum Elliptical States in the Coulomb Potential

Michael G.A. Crawford  
 Laboratory of Atomic and Solid State Physics,  
 Cornell University, Ithaca, NY, 14853-2501

A special relativistic perturbation to non-relativistic quantum mechanics is shown to lead to the special relativistic prediction for the rate of precession for quantum states in the Coulomb potential. This behavior is illustrated using SO(4) coherent states as examples. These states are localized on Kepler ellipses and precess in the presence of a relativistic perturbation.

## I. INTRODUCTION

Classical objects which are bound by forces which vary by the inverse square of distance have elliptical orbits whose orientation does not change with time. It is well known that the inclusion of relativistic effects causes these elliptical orbits to precess. In the Coulomb potential, where interactions are electromagnetic, the rate of this precession is calculated using special relativity. This was first accomplished by Sommerfeld [1] who, for the purpose of calculating the fine structure of the hydrogen atomic spectrum in the old quantum theory, calculated the classical rate of precession due to a special relativistic treatment of the kinetic energy of a “spinless” electron the Coulomb potential. (Sommerfeld’s calculation ignored electron spin in part because it was not described until 1925 by Uhlenbeck and Goudsmit.)

Turning to quantum mechanics, relativistic behavior is here introduced as a perturbation to the non-relativistic Coulomb potential. To discuss this type of precession in quantum mechanics, the first requirement is a quantum mechanical orbit. Eigenstates of the unperturbed Hamiltonian are obvious candidates, but the standard states  $|n, \ell, m\rangle$  are certainly not elliptical. However, for this system there exist generalized coherent states which are localized along bound classical trajectories of arbitrary eccentricity [2]. These states are formed of the eigenstates pertaining to a single energy level and are hence themselves eigenstates of the Hamiltonian, stationary in time. With the introduction of a special relativistic perturbation, the states will change in time, and in the limit of large quantum number, should precess at the rate predicted by special relativity. As shown below, this is indeed the case.

## II. ESTIMATING THE RATE OF PRECESSION

In the non-relativistic theory, the unperturbed Hamiltonian is given by

$$\hat{H}_0 = \frac{\hat{p}^2}{2m} - \frac{Ze^2}{\hat{r}} \quad (2.1)$$

with energy eigenlevels

$$E_n^{(0)} = -mc^2 \frac{Z^2 \alpha^2}{2n^2}. \quad (2.2)$$

The perturbation to be considered is given by

$$\hat{H}_1 = -\frac{\hat{p}^4}{8m^3c^2} \quad (2.3)$$

so that the first order Raleigh-Schrödinger perturbative correction to the energies is given by

$$E_{n,\ell}^{(1)} = -mc^2 \frac{Z^4 \alpha^4}{2n^3} \left( \frac{1}{\ell + \frac{1}{2}} - \frac{3}{4n} \right), \quad (2.4)$$

in which  $m$  is the electron mass,  $c$  is the speed of light,  $Z$  is the atomic number,  $\alpha = e^2/\hbar c$  is the fine structure constant,  $e$  is the electron charge,  $n$  is the total quantum number, and  $\ell$  is the quantum number pertaining to angular momentum, the eigenvalues of  $\hat{L}^2$  given by  $\hbar^2 \ell(\ell + 1)$ . The perturbation Eq. (2.3) is obtained by expanding the special relativistic expression for the kinetic energy and retaining the next term after the Newtonian term. No spin-orbit coupling is considered in parallel to the classical theory to which these calculations will be compared.

The classical period may be extracted from the quantum spectrum Eq. (2.2) as follows. The expansion of the energy eigenlevels about  $n = \langle n \rangle$  is given by

$$E_n^{(0)} = -mc^2 \frac{Z^2 \alpha^2}{2} \left( \frac{1}{\langle n \rangle^2} + \frac{2}{\langle n \rangle^3} (n - \langle n \rangle) - \frac{3}{\langle n \rangle^4} (n - \langle n \rangle)^2 + O((n - \langle n \rangle)^3) \right). \quad (2.5)$$

Now assume that the system is in some state  $|\psi\rangle$  with average total quantum number  $\langle n \rangle$  and uncertainty  $(\Delta n)^2 = \langle n^2 \rangle - \langle n \rangle^2$ . If the quantum time evolution is expressed in terms of the eigenstate expansion,

$$|\psi(t)\rangle = \sum_n e^{-iE_n t/\hbar} c_n |n\rangle, \quad (2.6)$$

the first term in Eq. (2.5) leads to an overall phase factor which may be dropped, and the second term will lead to phase factors that are integer multiples of  $2\pi$  when

$$t = T_{cl} = \frac{2\pi \hbar^3 \langle n \rangle^3}{m Z^2 e^4}. \quad (2.7)$$

This gives the classical period of a classical trajectory with energy  $E_n^{(0)}$  exactly, a circumstance closely connected to the success of Bohr-Sommerfeld quantization in hydrogenic atoms. Also, for hydrogenic wave functions, radial expectation values are given by

$$r_n = \langle n, \ell, m | \hat{r} | n, \ell, m \rangle = \frac{n^2 \hbar^2}{Z m e^2}. \quad (2.8)$$

Substitution of this value into  $T_{cl}$  yields

$$T_{cl}^2 = \frac{4\pi^2 r_n^3}{Z^4 e^4}, \quad (2.9)$$

a quantum rendering of Kepler's third law.

If the expansion Eq. (2.5) terminated with the linear term, then periodic motion would continue indefinitely. However, the quadratic and higher terms contribute a dephasing influence and the approximation of periodic behaviour eventually breaks down. To estimate the size of this dephasing influence, evaluate the quadratic term at the edge of the distribution in  $n$  ( $n = \langle n \rangle \pm \Delta n$ ) at  $t = T_{cl}$  to yield the "test quantity"

$$\delta\phi = 3\pi \frac{(\Delta n)^2}{\langle n \rangle}. \quad (2.10)$$

Hence, in the special case of a state localized in position and momentum, Ehrenfest's equations indicate an initial trajectory which follows a classical trajectory. In the additional case that  $\delta\phi \ll 2\pi$ , the state achieves at least a full period of behavior approximating classical behavior. These considerations are similar to those used employed in describing wave function revivals [3–6].

Now treating the relativistic perturbation to kinetic energy Eq. (2.4) in a similar manner, the expansion about  $\ell = \langle \ell \rangle$  of the perturbation Eq. (2.4) is given by

$$E_{n,\ell}^{(1)} = mc^2 \frac{Z^4 \alpha^4}{2n^3} \left[ - \left( \frac{1}{\langle \ell \rangle + \frac{1}{2}} - \frac{3}{4n} \right) + \frac{(\ell - \langle \ell \rangle)}{(\langle \ell \rangle + \frac{1}{2})^2} - \frac{(\ell - \langle \ell \rangle)^2}{(\langle \ell \rangle + \frac{1}{2})^3} + O((\ell - \langle \ell \rangle)^3) \right]. \quad (2.11)$$

Suppose the system is now in a state composed of eigenstates pertaining to the same  $n$ , degenerate in the unperturbed system. Then, the term independent of  $(\ell - \langle \ell \rangle)$  in Eq. (2.11) leads to overall phase factors, and the linear term leads to integer multiples of  $2\pi$  when

$$t = T_p = \frac{4\pi \hbar n^3}{mc^2 Z^4 \alpha^4} \left( \langle \ell \rangle + \frac{1}{2} \right)^2. \quad (2.12)$$

This may be written in terms of  $T_{cl}$ , yielding

$$T_p = \frac{2T_{cl}}{Z^2 \alpha^2} \left( \langle \ell \rangle + \frac{1}{2} \right)^2. \quad (2.13)$$

Note that  $T_p \gg T_{cl}$  which follows from  $E_{n,\ell}^{(1)} \ll E_n^{(0)}$ .

With the additional assumption that the system is in a state built up upon a particular classical orbit (such states are described in the next section), the evolution which occurs on a time scale  $T_p$  derived above must be of the same nature as classical precession due to relativity, that is, in-plane rotation of the state about the origin with a period of  $T_p$ . If this is the case, then the angle of rotation per classical period  $T_{cl}$  is given by

$$\delta\omega = \frac{\pi Z^2 \alpha^2}{(\langle \ell \rangle + \frac{1}{2})^2}. \quad (2.14)$$

Continuing the analogous arguments which lead to Eq. (2.10), the quadratic term of Eq. (2.11) evaluated at  $t = T_p$  at the edges of the distribution in  $\ell$  yields the test quantity

$$\delta\phi = \frac{mc^2 Z^4 \alpha^4 (\Delta\ell)^2 T_p}{2n^3 (\langle \ell \rangle + \frac{1}{2})^3 \hbar} = \frac{2\pi (\Delta\ell)^2}{\langle \ell \rangle + \frac{1}{2}}. \quad (2.15)$$

Again, if  $\delta\phi$  is small, then the state at  $t = T_p$  will approximately resemble the state at  $t = 0$ . This condition is best satisfied by Rydberg states with large angular momentum.

From Bergmann [7], the classical rate of perihelion precession according to special relativity is given by<sup>1</sup>

$$\delta\omega = \pi \frac{G^2 M^2 m^2}{c^2 L^2}, \quad (2.16)$$

measured as a change in angle per classical period of the vector pointing from perihelion to aphelion. In this expression,  $G$  is the gravitational constant,  $M$  is the (large) mass of the source of the gravitational field,  $m$  is the (small) mass of body in orbit, and  $L$  is the orbital angular momentum of the orbiting body. To compare the quantum prediction Eq. (2.14) with the classical rate Eq. (2.16), replace the strength of the Coulomb potential ( $Ze^2$ ) with that of the Kepler problem ( $GMm$ ), and note that the total angular momentum squared will be close to  $\hbar^2 (\langle \ell \rangle + \frac{1}{2})^2$  given the above assumptions that  $\langle \ell \rangle$  is large and  $(\Delta\ell)^2$  is small:

$$\langle \ell(\ell + 1) \rangle - (\langle \ell \rangle + \frac{1}{2})^2 = (\Delta\ell)^2 - \frac{1}{4}. \quad (2.17)$$

These substitutions render the quantum estimate Eq. (2.14) identical to Eq. (2.16) as anticipated.

---

<sup>1</sup>This rate is never observed in nature since those objects whose orbits are observed to precess are invariably gravitationally bound, requiring a general relativistic treatment. Such a treatment yields a rate, observed in the case of Mercury [8], of  $\delta\omega = 6\pi G^2 M^2 m^2 / c^2 L^2$ .

### III. SO(4) COHERENT STATES

The generalization of coherent states due to Perelomov [9,10] is useful in this context. This generalization rests upon the group structure of the system in question. In the case of the hydrogen atom, the dynamical group is SO(4,2) [11–13]. For the present purposes, it is not necessary to engage the entire group; the degeneracy group SO(4) contains sufficient structure. Treatments of coherent states of this description are existent in the literature [2,6].

The realization of SO(4) which describes the degeneracy of the hydrogen atom spectrum is given by the elements of the angular momentum operator and those of the scaled Laplace-Runge-Lenz vector. Given a classical orbit, the classical version of the Laplace-Runge-Lenz vector is proportional in magnitude to the eccentricity and is aligned parallel to the major axis. The corresponding quantum operators in atomic units are given by [13]

$$\hat{\mathbf{L}} = \hat{\mathbf{r}} \times \hat{\mathbf{p}}, \quad (3.1)$$

$$\hat{\mathbf{A}} = \frac{1}{2}\hat{\mathbf{r}}\hat{p}^2 - \hat{\mathbf{p}}(\hat{\mathbf{r}} \cdot \hat{\mathbf{p}}) - \frac{1}{2}\hat{\mathbf{r}}. \quad (3.2)$$

All of these operators commute with the Hamiltonian, leading to conservation of these quantities under time evolution. Conservation of angular momentum is to be expected in this (spherically symmetric) potential, but conservation of the  $\hat{\mathbf{A}}$  (a simple derivation of which is given by Wulfman [14]) is a unique property of the non-relativistic Coulomb potential. The classical interpretation of the invariance of the Laplace-Runge-Lenz vector is that elliptical orbits do not precess.

These operators satisfy the commutation relations

$$[\hat{L}_j, \hat{L}_k] = i\epsilon_{jkl}\hat{L}_l, \quad [\hat{A}_j, \hat{A}_k] = i\epsilon_{jkl}\hat{L}_l, \quad [\hat{L}_j, \hat{A}_k] = i\epsilon_{jkl}\hat{A}_l. \quad (3.3)$$

These six operators may be decoupled into two groups of three operators via

$$\hat{M}_j = \frac{1}{2}(\hat{L}_j + \hat{A}_j), \quad \hat{N}_j = \frac{1}{2}(\hat{L}_j - \hat{A}_j), \quad (3.4)$$

which commute according to

$$[\hat{M}_j, \hat{M}_k] = i\epsilon_{jkl}\hat{M}_l, \quad [\hat{N}_j, \hat{N}_k] = i\epsilon_{jkl}\hat{N}_l, \quad [\hat{M}_j, \hat{N}_k] = 0. \quad (3.5)$$

In terms of these new operators, it is clear that SO(4) = SO(3)  $\otimes$  SO(3).

The group SO(4) has two Casimir operators, given by

$$\hat{C}_1 = \hat{L}^2 + \hat{A}^2 = 2(\hat{M}^2 + \hat{N}^2), \quad (3.6)$$

$$\hat{C}_2 = \hat{\mathbf{L}} \cdot \hat{\mathbf{A}} = \hat{M}^2 - \hat{N}^2. \quad (3.7)$$

In the hydrogenic realization of this group,  $\hat{C}_2 = 0$  so that quantum mechanically and classically, angular momentum is perpendicular to the Laplace-Runge-Lenz vector. The second Casimir operator also indicates that the dimensions of the irreducible representations of the SO(3) generated by the  $\hat{M}_k$  and by the  $\hat{N}_k$  are equal (say, to  $n = 2j + 1$ ) so that the dimensions of the relevant unitary irreducible representations of SO(4) are  $n^2$ , the famous degeneracy of the hydrogen atom energy spectrum. Thus the first Casimir operator is equal to

$$\hat{C}_1 = 4j(j + 1) = n^2 - 1, \quad (3.8)$$

representing a constraint on the sum  $\langle \hat{L}^2 + \hat{A}^2 \rangle$ .

Turning to the SO(4) coherent states, Since SO(4) = SO(3)  $\otimes$  SO(3), the SO(4) coherent states may be expressed as the direct product of two SO(3) coherent states which are themselves standard in the literature [15,10,16]. The SO(3) coherent states are given by

$$|j, \zeta\rangle = \sum_{m=-j}^j \left( \frac{(2j)!}{(j+m)!(j-m)!} \right)^{1/2} \frac{\zeta^{j+m}}{(1+|\zeta|^2)^j} |j, m\rangle, \quad (3.9)$$

parameterized by the complex valued  $\zeta$ . In these states, expectation values of the angular momentum operators are given by

$$\langle \hat{\mathbf{J}} \rangle = \frac{2j}{1+|\zeta|^2} \left( \text{Re}(\zeta), -\text{Im}(\zeta), \frac{1}{2}(|\zeta|^2 - 1) \right), \quad (3.10)$$

with  $\hat{\mathbf{J}}$  standing for  $\hat{\mathbf{M}}$  or  $\hat{\mathbf{N}}$  as the case may be. With these expressions in mind, the SO(4) coherent states are given by

$$|n, \zeta_1, \zeta_2\rangle = |j, \zeta_1\rangle |j, \zeta_2\rangle. \quad (3.11)$$

Here,  $n = 2j + 1$ , and  $\zeta_1$  and  $\zeta_2$  parameterize the SO(3) coherent states pertaining to  $\hat{\mathbf{M}}$  and  $\hat{\mathbf{N}}$  respectively. The expectation values of the angular momentum and Laplace-Runge-Lenz operators may be regained through Eq. (3.10) and the relations  $\hat{\mathbf{L}} = \hat{\mathbf{M}} + \hat{\mathbf{N}}$  and  $\hat{\mathbf{A}} = \hat{\mathbf{M}} - \hat{\mathbf{N}}$ . (The substitution of Eq. (3.9) into Eq. (3.11) yields a double sum over the direct product states  $|j, m_1\rangle |j, m_2\rangle$ . These states may be calculated by relating them to the standard hydrogenic eigenstates  $|n, \ell, m\rangle$  via the Clebsch-Gordon coefficients.)

For the purpose of visualization, spherical symmetry permits setting  $\langle \hat{\mathbf{L}} \rangle$  parallel to the  $z$ -axis, achieved by setting  $\zeta_2 = -\zeta_1$ . Since  $\hat{\mathbf{L}} \cdot \hat{\mathbf{A}} = 0$ , the vector  $\langle \hat{\mathbf{A}} \rangle$  may be oriented parallel to the  $x$ -axis accomplished by setting the imaginary parts of  $\zeta_1$  and  $\zeta_2$  equal to zero. These identifications reduce the problem to the variation of a single real parameter, say  $\eta = \text{Re}(\zeta_1)$ . In terms of this parameter, expectation values are given by

$$\langle \hat{L}_3 \rangle = \frac{2j(\eta^2 - 1)}{1 + \eta^2}, \quad \langle \hat{A}_1 \rangle = \frac{4j\eta}{1 + \eta^2}. \quad (3.12)$$

With the magnitude of the classical Laplace-Runge-Lenz vector being proportional to the eccentricity  $\epsilon$  of the orbit, the quantum calculation leads to

$$\epsilon = \frac{2\eta}{1 + \eta^2}. \quad (3.13)$$

Also in terms of  $\eta$ , the total angular momentum may be expressed as

$$\langle \hat{L}^2 \rangle = 2j(j+1) + 2j^2 \frac{\eta^4 - 6\eta^2 + 1}{(1 + \eta^2)^2}. \quad (3.14)$$

This expression follows from  $\langle \hat{L}^2 \rangle = \langle (\hat{\mathbf{M}} + \hat{\mathbf{N}}) \cdot (\hat{\mathbf{M}} + \hat{\mathbf{N}}) \rangle$ , Eq. (3.10), and  $\langle \hat{\mathbf{M}} \cdot \hat{\mathbf{N}} \rangle = \langle \hat{\mathbf{M}} \rangle \cdot \langle \hat{\mathbf{N}} \rangle$ , the last of which since  $[\hat{M}_j, \hat{N}_k] = 0$ .

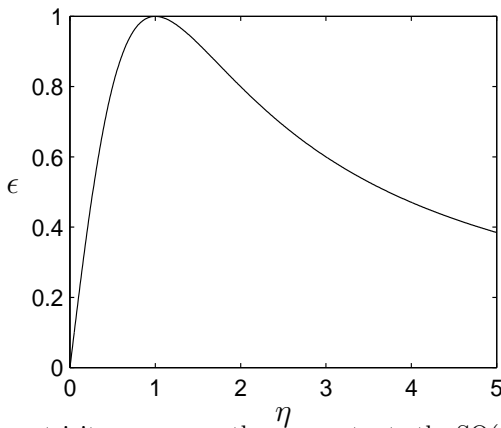


FIG. 1. Eccentricity  $\epsilon$  versus  $\eta$ , the parameter to the SO(4) coherent state.

By virtue of their construction, the SO(4) coherent states are minimum uncertainty states of rotated 4-dimensional angular momentum operators. One therefore expects that for moderate 4-dimensional rotations, the states will remain localized in angular momentum and in the Laplace-Runge-Lenz vector, that is, localized about a particular classical orbit. Hence, given a value of  $\eta$ , the approximate geometry is given by Eq. (3.13), with a semi-major axis given by Eq. (2.8).

#### IV. PRECESSING COHERENT STATES

The value of the test quantity  $\delta\phi$  given by Eq. (2.15) is expressible in terms of the SO(4) coherent state parameter  $\eta$ . With expectation values taken in an SO(3) coherent state,

$$(\Delta \hat{J}_3)^2 = 2j \frac{\eta^2}{(1 + \eta^2)^2}, \quad (4.1)$$

and

$$(\Delta \ell)^2 = (\Delta \hat{L}_3)^2 = (\Delta \hat{M}_3)^2 + (\Delta \hat{N}_3)^2, \quad (4.2)$$

since  $\hat{M}_j$  and  $\hat{N}_j$  commute. With these in mind, and dropping the  $\frac{1}{2}$  from the denominator of  $\delta\phi$  since  $\langle \ell \rangle$  is large,

$$\delta\phi = 2\pi \frac{\eta^2}{\eta^4 - 1}. \quad (4.3)$$

Therefore, in the sense that  $\delta\phi = 0$ , the precession is best for  $\eta = 0$  or as  $\eta \rightarrow \infty$ . In both cases, though, from Eq. (3.13), the resultant orbits will be circular and no precession can be observed: There is a certain tradeoff between the observability and “coherence” of the precession measured by  $\delta\phi$ . In fact, it is convenient to express  $\delta\phi$  in terms of  $\epsilon$  from Eq. (3.13) so as to connect this test with a more physical or geometrical quantity:

$$\delta\phi = \frac{2\pi\epsilon^2(2 - \epsilon^2 \pm 2\sqrt{1 - \epsilon^2})}{8 - 8\epsilon^2 \pm 4(2 - \epsilon^2)\sqrt{1 - \epsilon^2}} = \frac{\pi}{2}\epsilon^2 + O(\epsilon^4), \quad (4.4)$$

where the positive sign is appropriate for  $\eta > 1$  and the negative for  $\eta < 1$ . As shown in Figure 2, as the eccentricity increases, the degree to which the wave functions remain assembled decreases.

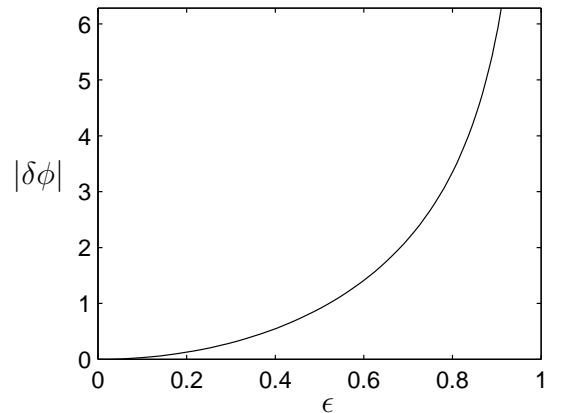


FIG. 2. Test parameter  $\delta\phi$  versus eccentricity  $\epsilon$ .

For some examples of precessing coherent states, examine Figure 3. This figure depicts a mesh plot of an SO(4) coherent state at  $t = 0$ , and a sequence of overlaid contour plots showing states precessed from  $t = 0$  to  $t = \frac{1}{4}T_p$ . To appreciate the physical scale of these simulations, the field of view in all cases is  $4.23 \mu\text{m}$  across and with states in the 141st energy level, the classical period is  $4.25 \times 10^{-10}$  seconds. In Figure 3(b), with  $\epsilon = 0.385$ , the precession period is 0.266 seconds or  $6.26 \times 10^8$  classical periods, which on atomic scales, is a very long time. In the subsequent images, the rate of precession is larger owing to the larger eccentricity so that the precession period of the state depicted in Figure 3(d) is 0.164 seconds. This interval is still much longer than the longest times Rydberg states are observed in experimental setups, typically 1 nanosecond [5].

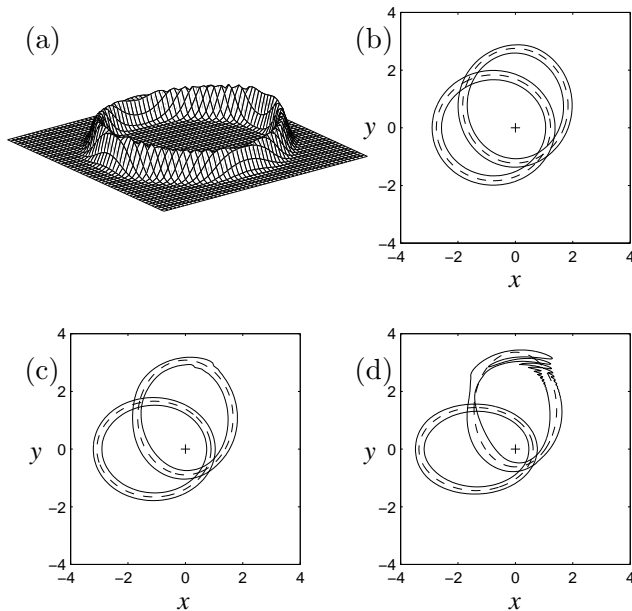


FIG. 3. Some examples of precessing  $SO(4)$  coherent states: (a) In the 141st energy level, at  $t = 0$ , with  $\eta = 0.2$  (or  $\epsilon = 0.385$ ) on the  $x$ - $y$  plane with amplitude proportional to  $|\langle \mathbf{r} | \mathbf{141}, \zeta_1, \zeta_2 \rangle|^2$ . (b) The same state as (a), with position plotted in  $10^4$  atomic units, and the origin located at the  $+$  symbol. The state at  $t = 0$  is oriented horizontally, and  $t = \frac{1}{4}T_p$  oriented vertically. The solid lines depict a single contour on the quantum wave function, and the dashed lines depict the classical orbit precessed according to the special relativistic prediction. (c) The same as (b), but with  $\eta = 0.3$  (or  $\epsilon = 0.550$ ). (d) The same as (b), but with  $\eta = 0.4$  (or  $\epsilon = 0.690$ ).

As apparent from the images, the quantum rate of precession agrees with the classical special relativistic prediction. In the case of Figure 3(b), though only shown until  $t = \frac{1}{4}T_p$ , the state remains localized on the ellipse up to the full period of the precession. Not surprisingly, for increased eccentricities, the degree of “coherence” of the state decreases, leading to the decay of the state as depicted in Figure 3(d) after only a quarter precession period.

## V. CONCLUSIONS

The perturbation Eq. (2.3) was chosen so that a direct comparison could be made between the quantum mechanical calculation and the special relativistic calculation due to Sommerfeld. Therefore, spin effects were ignored which are equal in size to the kinetic energy perturbation. This means that the quantities calculated here are not predictions to be tested in the laboratory. The purpose has been to show that a simple analysis of a quantum perturbation can reproduce the results of

a more involved classical analysis. In particular, a special relativistic perturbation to non-relativistic quantum mechanics leads to an agreement with classical special relativity in a large quantum number limit. A similar notion of agreement may be found in the work of McRae and Vrscay [17] who have studied correspondence between quantum and classical perturbation schemes. In their work, as well as in the present paper, it transpires that the simplest route to the determination of a classical perturbation may be through the classical limit of a quantum perturbation.

## VI. ACKNOWLEDGMENTS

This work was supported by the Natural Sciences and Engineering Research Council of Canada, and the National Science Foundation. The author would also like to acknowledge useful discussions with Prof. N.W. Ashcroft of the Department of Physics, Cornell University, and Profs. E.R. Vrscay and J. Paldus of the Department of Applied Mathematics, University of Waterloo.

- 
- [1] A. Sommerfeld. *Atombau und Spektrallinien*. F. Vieweg und Sohn, Braunschweig, Germany, 1921.
  - [2] J.C. Gay, D. Delande, and A. Bommier. Atomic quantum states with maximum localization of classical elliptical orbits. *Phys. Rev. A*, 39(12):6587–6590, 1989.
  - [3] I.S. Averbukh and N.F. Perelman. Fractional revivals: Universality in the long-term evolution of quantum wave packets beyond the correspondence principle dynamics. *Phys. Lett. A*, 139(9):449–453, 1989.
  - [4] M. Nauenberg. Autocorrelation function and quantum recurrence of wavepackets. *J. Phys. B*, 23:L385–L390, 1990.
  - [5] J.A. Yeazell, M. Mallalieu, and Jr. C.R. Stroud. Observation of the collapse and revival of a Rydberg electronic wave packet. *Phys. Rev. Lett.*, 64(17):2007–2010, 1990.
  - [6] M.G.A. Crawford. Temporally stable coherent states in energy degenerate systems: The hydrogen atom. *Phys. Rev. A*, 62(1):012104–1–7, 2000.
  - [7] G. Bergmann. *Introduction to the Theory of Relativity*. Prentice-Hall, Englewood Cliffs, NJ, 1942.
  - [8] C.M. Will. *Theory and Experiment in Gravitational Physics*. Cambridge University Press, Cambridge, revised edition, 1993.
  - [9] A.M. Perelomov. Coherent states for arbitrary Lie groups. *Commun. Math. Phys.*, 26:222–236, 1972.
  - [10] A.M. Perelomov. *Generalized Coherent States and Their Applications*. Springer-Verlag, London, 1986.
  - [11] A.O. Barut and G.L. Bornzin.  $SO(4,2)$ -Formulation of the symmetry breaking in relativistic Kepler problems with or without magnetic charges. *J. Math. Phys.*, 12(5):841–846, 1971.

- [12] J. Paldus. Dynamical groups. In G.W.F. Drake, editor, *Atomic, Molecular and Optical Physics Handbook*. AIP Press, Woodbury, New York, 1996.
- [13] B.G. Adams, J. Čížek, and J. Paldus. Lie algebraic methods and their applications to simple quantum systems. In *Advances in Quantum Chemistry, Vol 19*. Academic Press, New York, 1988.
- [14] C.E. Wulfman. Dynamical groups in atomic and molecular physics. In E.M. Loeb, editor, *Group Theory and Its Applications*, volume II. Academic Press, New York, 1971.
- [15] J.R. Klauder and B.-S. Skagerstam, editors. *Coherent States: Applications in Physics and Mathematical Physics*. World Scientific, Singapore, 1985.
- [16] W.-M. Zhang, D.H. Feng, and R. Gilmore. Coherent states: Theory and some applications. *Rev. Mod. Phys.*, 62(4):867–927, 1990.
- [17] S.M. McRae and E.R. Vrscaj. Perturbation theory and the classical limit of quantum mechanics. *J. Math. Phys.*, 38(6):2899, 1997.